DOI: 10.1002/ejoc.200800247

A Chiral "Frozen" Hydrogen Bonding in C_4-Symmetric Inherently Chiral Resorcin[4]arenes: NMR, X-ray, Circular Dichroism, and Theoretical Study

Bogumił Kuberski,[a] Magdalena Pecul,[b] and Agnieszka Szumna*[a]

Keywords: Calixarenes / Amino acids / Atropisomerism / Conformation analysis / Receptors

Chiral C_4-symmetric resorcinarenes, substituted with L-amino acid derivatives at upper rims, were synthesized by the modified Mannich reaction and subsequent *N*-substitution reactions. Compounds of that type (**5a**–**e**) can exist in two relatively stable inherently chiral C_4-symmetric conformations, (*M*) and (*P*), stabilized by the formation of seams of hydrogen bonds. However, because of diastereomeric preferences the amino acid substituted resorcinarenes exhibit considerable diastereomeric excesses for the induced conformational inherent chirality (up to ≥95 %). The relatively slow exchange allowed the determination of the directions of the hydrogen bond ring closures through the combined application of NMR (ROESY) and X-ray analysis. It was also possible to correlate the absolute conformation with the sign of the Cotton effects observed for the transitions within the resorcinol chromophore in the CD spectra (solution and solid state). The ab initio calculations (TDDFT/B3LYP/DZVP and TDDFT/CAMB3LYP/6-31++G*) for model compounds showed that the chiral arrangement of the hydrogen bonding in resorcinarenes can produce substantial CD effects, which are amplified by exciton coupling. However, it was also shown that the neighboring urea, amide, or phenyl groups have crucial effects on the direction of electric transition dipoles and, as the result, on the signs of the exciton-coupled bands.

Introduction

The majority of large proteins in cells are symmetrical oligomeric complexes with two or more subunits. Such symmetrical arrangements have many advantages that justify their evolutionary selection.[1] The advantages involve error control in synthesis, coding efficiency, and cooperative functions such as allosteric binding, assembly, and amplification of the molecular response to external stimuli.[2] Symmetrical synthetic molecules also have similar advantages that include simplified synthesis and the possibility of amplification of molecular properties through symmetrical supramolecular organization. These features make them useful in many areas including catalysis, molecular recognition, and material science. Of special interest are molecules possessing only rotational symmetry, which proved to be effective as asymmetric catalysts[3] or chiral materials.[4] Examples are widely known for C_2- and C_3-symmetric molecules,[3] whereas there is comparatively less known about chiral systems possessing higher rotational symmetry.

The promising but still relatively poorly explored class of chiral molecules having rotational symmetry are those exhibiting inherent chirality.[5] Recently, our group[6] and others[7] reported chiral C_4-symmetric organization of the arms of resorcin[4]arenes by means of the cooperative belts of hydrogen bonds. Compounds of type **1** (Scheme 1) can exist in two C_4-symmetric enantio/diastereomeric conformations, (*M*) and (*P*), and can switch between those two forms with the concerted rupture of eight stabilizing hydrogen bonds (and thus exhibiting considerable energetic barriers).[6] The examples of the determination of the stereochemistry of covalently inherently chiral resorcinarenes are limited[5a,8] and for the conformationally inherently chiral compounds the task was so far not feasible due to the timescale of the relatively fast dynamic processes. In the current paper we show the effective synthesis of C_4-symmetric conformationally inherently chiral resorcinarenes **5a**–**e**, substituted with L-amino acid derivatives, and for the first time, we address the question of their stereochemistry. We hoped that by using amino acids as upper rim substituents, in addition to providing the source of chirality to promote differentiation of diastereomeric conformers, may provide additional stabilizing interactions (hydrogen bonding and/or steric overcrowding) to slow down the dynamic processes and thus allow the determination of the direction of the hydrogen bond ring closures.

Additionally, we would like to discuss the correlation between asymmetry of the hydrogen bonding system and the chiroptical spectra. We previously noted interesting circular dichroism spectra for the compounds of type **1**, which have

[a] Institute of Organic Chemistry, Polish Academy of Sciences, Kasprzaka 44/52, 01-224 Warsaw, Poland
Fax: +48-22-632-6681
E-mail: szumnaa@icho.edu.pl
[b] Department of Chemistry, Warsaw University, Pasteura 1, 02-093 Warsaw, Poland

Supporting information for this article is available on the WWW under http://www.eurjoc.org or from the author.

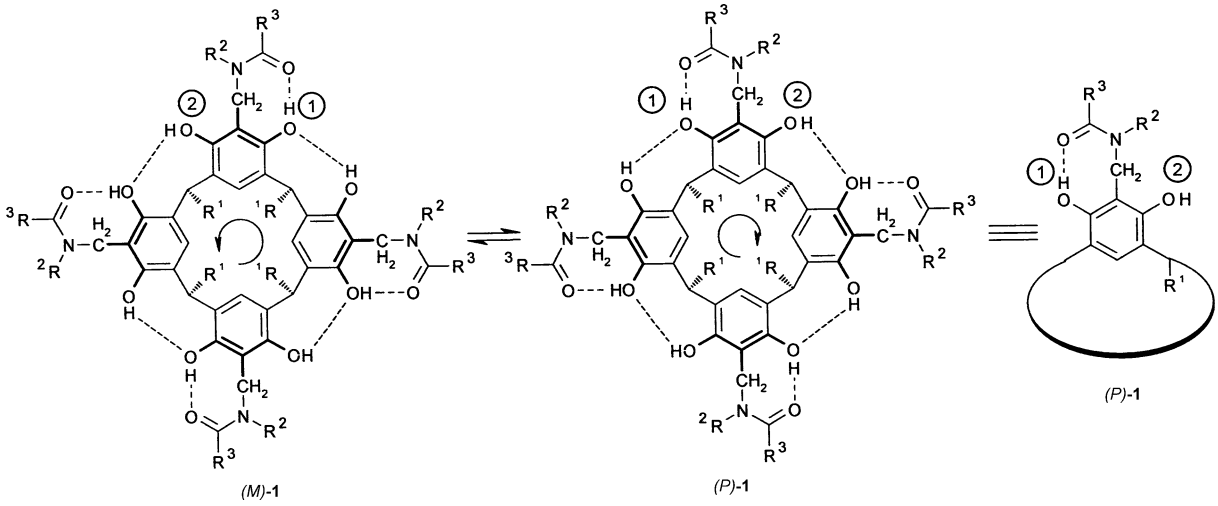

Scheme 1. Structure and stereochemical notation of conformationally inherently chiral resorcin[4]arenes.

shown considerable Cotton effects in the region of the absorption of the resorcinarene skeleton − quite remote from the chiral centers, but involved in the conformationally chiral pattern.[6] The question arises as to whether the Cotton effects can be ascribed to the "frozen" chiral hydrogen bonding system involving the resorcinarene chromophore or to other more elusive factors. In order to shed light on these questions we preformed ab initio calculations for the model compounds and discussed the application of the exciton chirality method for the current systems.

Results and Discussion

Synthesis

The Mannich reaction between resorcin[4]arene **2**, formaldehyde, and primary amines in methanol is known to give tetrabenzoxazines of type **3** (Scheme 2).[5c] Application of such a procedure for L-amino acid methylamides gave benzoxazines **3a** and **3b**. In order to obtain secondary amines **4** the N,O-acetal bridge of **3** had to be removed. Recently, we reported mild conditions for N,O-acetal removal by using ethyl nitroacetate.[6] That procedure was very efficient and worked also for amino acid derivatives **3a** and **3b**. However, the simplification of the procedure by applying the direct route (Scheme 2, route c) would be desirable. A little puzzling is that examples of the isolation of intermediate secondary amines of type **4** from the direct route are not known. To check the possibility of formation of amine **4b** through the direct route we initially modified the known "benzoxazine" procedure by simply changing the ratio of the reagents from 1:5:10 to 1:4:4 (**2**/amine/HCHO) in MeOH/AcOH. The reaction gave a complicated mixture of differently substituted amines and benzoxazines, which were very difficult to separate. As a result, we obtained amine **4b** in low yield (≈20%). During the course of the optimization we found that substantial modification of the original procedure by (1) changing the solvent from methanol to dichloromethane (the reaction is then two phase), (2) changing the ratio of the reagents to 1:5:4 (**2**/amine/

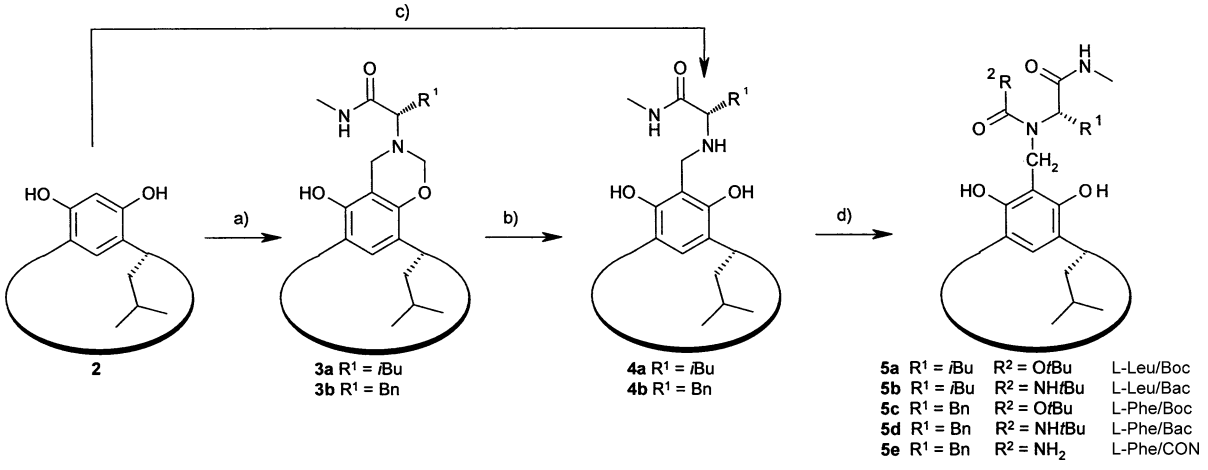

Scheme 2. Synthesis of **5a**–**e**. Reagents and conditions: (a) aq. HCHO, L-amino acid methylamide, AcOH, MeOH; (b) ethyl nitroacetate, MeOH; (c) aq. HCHO, L-amino acid methylamide, CH_2Cl_2; (d) see Experimental Section.

HCHO), and (3) using no acid allowed the synthesis of amines **4a** and **4b** in high yields (64–76%). Moreover, the mixtures were much easier to separate, in the case of **4b** just by filtration.

The subsequent *N*-substitution reactions resulting in final products **5a**–**e** were carried out in analogy to the previously described procedures[6] by using di-*tert*-butyl dicarbonate (for **5a**, **5c**), *tert*-butyl isocyanate (for **5b**, **5d**), or trimethylsilyl isocyanate (for **5e**). The reaction of trimethylsilyl isocyanate with amine **4a** gave the analogous product to **5e**; however, its solubility in common organic solvents was too low for further studies.

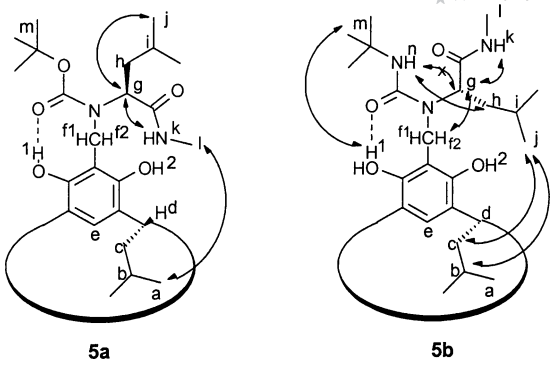

Figure 1. The most relevant ROESY contacts for **5a** and **5b**.

The Dynamics and Stereochemistry of *tert*-Butoxycarbonyl (Boc) Derivatives 5a and 5c

^{1}H and ^{13}C NMR spectra in $CDCl_3$ for both L-Leu/Boc **5a** and L-Phe/Boc **5c** derivatives are relatively sharp and simplified by fourfold symmetry with the characteristic patterns for C_4-symmetric chiral conformations, namely, two distinct signals for the phenolic OH groups with a large chemical shift difference (see Supporting Information).

It was shown that the two diastereomeric conformations of the compounds of this type, being in the regime of slow exchange (NMR timescale), can be easily distinguished, as they have separate signals that exhibit chemical exchange cross peaks in the 2D EXSY experiments (moderate mixing time ca. 300 ms).[6] To probe the dynamics of **5a** and **5c**, we recorded 2D EXSY spectra in $CDCl_3$ by using various mixing times (ranging from 300 ms up to 1.5 s). In all cases no exchange was observed at 300 ms. Some exchange was observed at 1.5 s, but the integrals of the exchange cross peaks with respect to diagonal peaks are very small (and probably also biased by spin diffusion). This indicates that for amino acid derivatives **5a** and **5c** the isomerization is considerably slower than that of the previously reported derivatives of the simple aliphatic amines.

Because the dynamics of the system is slow (from EXSY experiments and the relatively sharp ^{1}H and ^{13}C spectra) and the second possible diastereomeric conformation is expected to have a considerably different spectrum, we postulate that Boc derivatives **5a** and **5c** exist in the solution as single diastereoconformers (*de* >95%).

The stereochemistry of **5a** and **5c** was probed by using ROESY spectra (τ_{mix} = 200 ms). For both derivatives, cross peaks were observed between methyl protons from the amino acid methylamide H^l and the methyl protons from the aliphatic lower rim of the resorcinarene skeleton H^a (Figure 1). This indicates that the molecule is highly bent with the backbone of the amino acid part pointing towards the bottom of the molecule. Such a bent structure implies that an amide moiety has to reside in close proximity to the aromatic walls, most probably by forming some kind of stabilizing amide···π[9] or amide···OH interactions.

The Stereochemistry of *tert*-Butylaminocarbonyl (Bac) Derivatives 5b and 5d

The ^{1}H NMR spectra of *tert*-butylaminocarbonyl (Bac) derivatives **5b** and **5d** in $CDCl_3$ contained multiple considerably broadened signals indicating the existence of numerous conformations. Although signals for one dominant conformation could be distinguished (having the features of C_4-symmetric conformation) the 2D spectra were uninformative due to overlapping signals. We have tried to influence the conformational equilibria by changing the solvent and the temperature. [D_8]Toluene spectra were even more complicated, and they simplified only at high temperatures (>363 K) showing C_4 symmetry. The [D_6]DMSO spectra of **5b** and **5d** showed single C_4-symmetric forms; however, the important signals were highly broadened (due to faster dynamic processes). Raising the temperature sharpened the signals, but the compounds appeared to be unstable (decomposition).

The reasonably sharp spectra at 303 K with one C_4-symmetric dominating form (>90%) was obtained for **5b** in 1,1,2,2-[D_2]tetrachloroethane ([D_2]TCE). The minor conformer was most probably an unsymmetrical form with one leucine side chain self-encapsulated in the cavity (interpreted from signals of leucine methyl groups at –0.4 and –1.9 ppm showing exchange peaks with each other and with analogous signals of the main conformer). The ROESY spectrum of **5b** (τ_{mix} = 200 ms, [D_2]TCE) revealed characteristic structural features of the main conformer. The most important cross peak is between the leucine methyl groups H^j and the aliphatic H^c and H^b protons from the aliphatic lower rim of the resorcinarene skeleton (Figure 1). This suggests that, contrary to the previous cases, it is the leucine side chain and not the backbone (as in the case of **5a**, **5c**, and **5e**) that is directed towards the lower rim of the resorcinarene. This implies that the aliphatic chains interact with the aromatic walls of the resorcinarene. Such a conclusion is also supported by the chemical shift of the leucine methyl protons H^j, which are high-field shifted and appear at δ = 0.4 ppm. Other important stereochemical information comes from the presence of a NH^n···H^{h1} contact in the absence of a NH^n···H^g contact, which indicates the proximity of the leucine side chain and the urea-type amide NH^n.

The molecular structure of **5b** in the solid state (X-ray, Figure 2) confirms the conclusions that were deduced from NMR spectroscopy. The molecule of **5b** is held in the inherently chiral conformation by means of 12 intramolecular hydrogen bonds (3 per unit). Analogous to the previously reported inherently chiral structures,[6,5d] the seam of hydrogen bonds is formed between the phenolic hydrogen atoms and the carbonyl groups (eight H-bonds). However, in the current structure, an additional four intramolecular hydrogen bonds are formed between urea-type NH^n groups and the carbonyl groups of the amino acid backbone (forming seven-membered rings). Another important intramolecular interaction is the CH···π interaction of the leucine methyl groups, which are directed towards the lower rim of the molecule and located in close proximity to the aromatic walls of the resorcinarene skeleton (Figure 2b, blue lines, C···aromatic plane distances ca. 3.7 Å). This explains the unusually low chemical shift for the methyl H^j protons in the ^{1}H NMR spectrum and justifies the H^j···H^c cross peaks in the ROESY spectrum. Also, the presence of NH^n–H^{h1} cross peaks (NH^n–H^{h1} distance is 2.0 Å) in the absence of NH^n···H^g contacts (distance 3.5 Å and spatial separation by a carbon atom) can be explained by the geometry of the molecule in the solid state. The methylamide H^l protons are in positions remote from the rest of the molecule, and this explains the absence of any ROESY cross peaks between them and other protons, except for trivial 1,3-contacts.

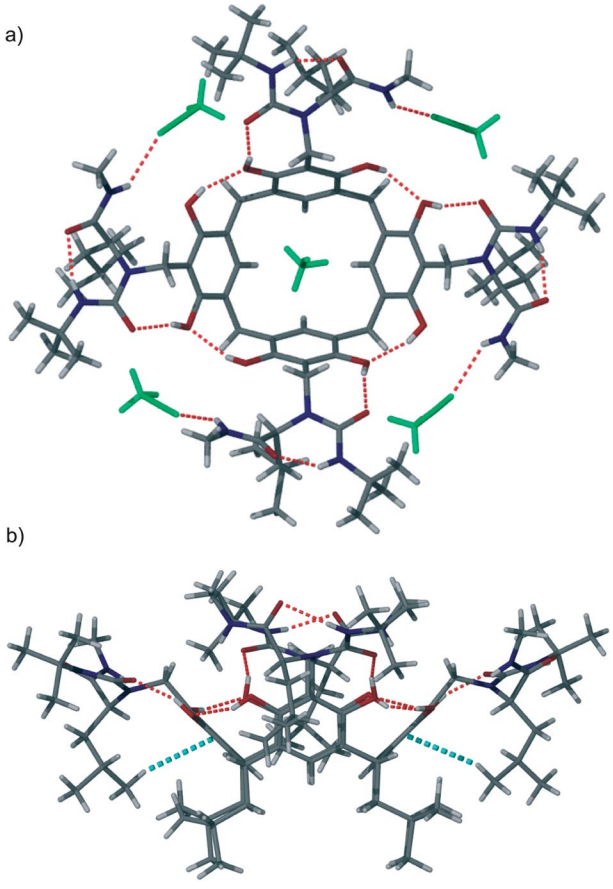

Figure 2. The crystal structure of **5b**: (a) top view; lower-rim alkyl chains were removed for clarity, MeCN solvent molecules are colored in green; b) side view; solvent molecules were removed for clarity, blue dotted lines represent close CH–π interactions.

While analyzing the crystal structure it is worth noting the extensive interactions of molecule **5b** with acetonitrile molecules. In the crystal structure, one acetonitrile molecule is hosted inside the molecular cavity and four others interact with the side chains through hydrogen bonding with the sixth molecule (occupancy 82%) found in the intermolecular voids. Another important feature is the slightly distorted *cone* conformation of the resorcinarene skeleton, which has an approximate noncrystallographic C_2 symmetry (distances between centroids of the opposite aromatic rings are 7.22 and 6.40 Å).

Because the configuration of L-leucine is known, it is possible to determine unambiguously the absolute structure of **5b** (and thus the conformation). We used the notation proposed by Heaney and coworkers[10] for chiral C_n-symmetric molecules with a slight modification for this noncovalent case (Scheme 1).[6] Thus, when looking from a position *above* the polar rim and by assuming that the doubly hydrogen bonded oxygen atom takes priority over the singly hydrogen-bonded oxygen atom, the stereochemistry of **5b** in the solid state can be described as (*P*). On the basis of the similarities, we postulate that the solution-state structure resembles the solid-state structure, and thus, the dominant conformation of **5b** in solution is also (*P*).

UV/CD Spectra

UV and circular dichroism (CD) spectra of the inherently chiral conformers **5a**–**e** are presented in Figure 3. For the current study, the spectral range 280–320 nm is of particular significance, as it is attributed to the transitions within the substituted resorcinol chromophore. The UV spectra of all products **5a**–**e** in chloroform exhibited absorption bands with similar wavelength maxima of 290 nm with pronounced low-energy shoulders at 309 nm. The band energy is not dependent on the type of amino acid (aromatic or aliphatic) or *N*-substituent (Bac, Boc, or CON). It was earlier postulated that these spectral characteristics come from the rigid C_4-cone conformation of the resorcinarene, which result in pronounced excitonic splitting of the individual ^1L_b electronic transitions.[11]

All CD spectra of compounds **5a**–**e** in $CHCl_3$ show the bisignate Cotton effects centered at almost identical wavelengths of 290 and 309 nm (Figure 3). In the case of the L-leucine derivatives, both Boc **5a** and Bac **5b** exhibited a negative CD couplet in the range of interest. The similar negative couplet was also observed for L-Phe/Boc **5c**. In contrast, L-Phe/Bac **5d** and L-Phe/CON **5e** exhibited a positive sign of the CD couplet.

Owing to the noncovalent nature of supramolecular interactions that are responsible for the inherently chiral arrangements, the medium and solvent interactions with the molecular components of the whole system can play a key role in such processes, thus influencing the degree of in-

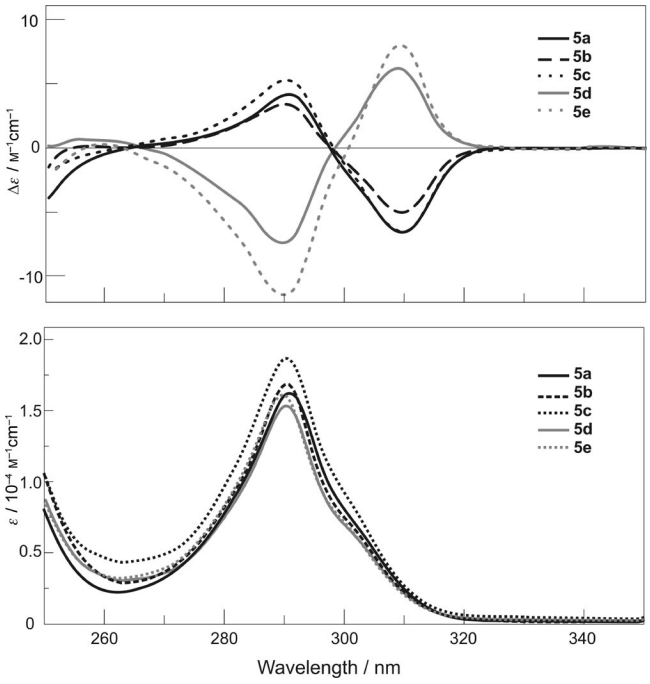

Figure 3. CD and UV spectra of **5a**–**e** ($CHCl_3$, 303 K).

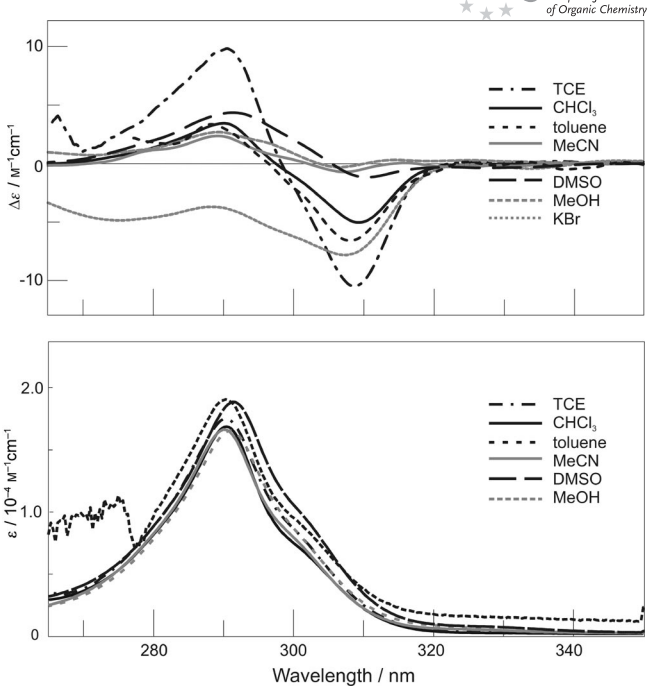

Figure 4. CD and UV spectra of **5b** in various solvents and in the solid state.

duced inherent chirality. To probe the solvent effects, we chose compound **5b**, for which the crystal structure is known. We recorded the CD spectra in various solvents and in a KBr matrix (Figure 4). The CD spectra revealed the strongest Cotton effects in TCE, which is in agreement with the NMR spectroscopic data, and showed that in that solvent the C_4-symmetric structure existed in the highest amount (for other derivatives there was no substantial difference between spectra in $CHCl_3$ and TCE). The spectra in more polar solvents (DMSO, MeCN, and MeOH) showed considerably smaller Cotton effects in the range of interest. It is also worth noting that the low-energy band (at 309 nm) is much more affected than the higher energy band (290 nm). This observation is in agreement with the previous observations for covalently inherently chiral resorcin[4]arenes, which also showed the decay of the low-energy band (309 nm) with increasing solvent polarity.[11] Surprisingly, the solid-state spectrum of **5b** exhibited only a monosignate negative Cotton effect at 309 nm. Although some flattening of the absorption bands is known for solid-state CD spectra,[12] it has a more unified character, so it can not be a reason for the selective one-band disappearance. We attribute this phenomenon to the lower symmetry of the resorcinarene skeleton in the solid state (C_2 *flattened-cone* conformation) than in the solution (C_4-*cone*). Such an interpretation is also supported by our previous observation of chiral resorcinarenes conformationally locked in *boat* conformations, which also showed monosignate Cotton effects.[13]

In order to gather more data for the current discussion, we recorded spectra of the crystals of the previously reported chiral resorcinarene **5f**.[6] In this case, the KBr sample exhibits the same sign and shape of the CD spectrum (positive bisignate Cotton effects) as in the $CHCl_3$ solution (Figure 5). Such an observation speaks in favor of our previous interpretation that the presence of excitonic splitting is strictly connected with the symmetry. The previously reported crystal structure of **5f** revealed an exact C_4-symmetric molecule (also crystallographic symmetry). The similarities of the spectra also allowed the assumption that a solid-state sample of **5f** exhibits the same conformation as those of the dominant form in solution.

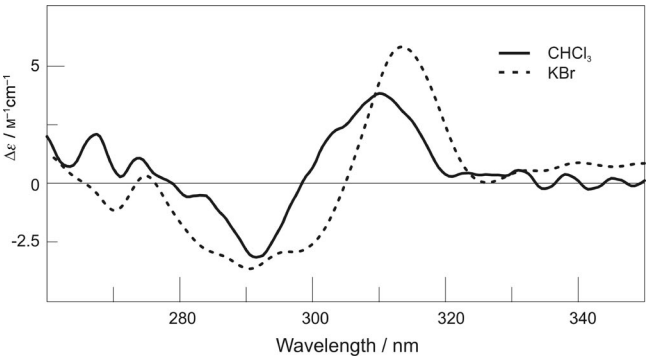

Figure 5. CD spectra of previously reported **5f**[6] ($CHCl_3$ solution and crystals in KBr).

On the basis of the NMR spectra and a crystal structure of **5b** (see previous section), we attribute the negative couplet in the 280–320 nm range to the structure with (*P*) arrangement of the hydrogen-bonding system. Surprisingly, for compound **5f**, the (*P*) arrangement of the hydrogen-bonding system (as in the crystal structure) is attributed to the positive couplet.

Discussion and the Ab Initio Calculations

We were particularly interested whether the chiral C_4-symmetrical arrangement of the hydrogen-bonding system is able to induce substantial CD signals for the transitions of the resorcinol chromophore. The subsequent question was if this arrangement is responsible for the sign of the experimentally observed Cotton effects for compounds **5a**–**e**. Those two questions are treated separately, because it is known that Cotton effects are sensitive to many factors (small conformational variations,[14] noncovalent interactions with nearby environment[15]) and thus the CD spectrum can be also influenced by those factors (very difficult to consider for such a large structure).

The simple but still accurate approach to the interpretation of CD spectra of multichromophoric systems consists in application of the exciton coupling theory.[16] Although the CD spectra are almost routinely recorded for inherently chiral compounds as a proof of their chirality, the examples of data interpretation by application of excitonic coupling are very limited.[11,5a] In order to consider the applicability of that theory to the C_4-symmetric resorcin[4]arenes, we focus on the influence of structural features on the direction of electric dipoles.

For the resorcinol chromophore, the lowest ^1L_b state is of interest. For C_{2v}-symmetric resorcinol, the electric-transition dipole is polarized in the plane of the aromatic ring (Figure 6a). Its direction can be turned by differentiation of the OH groups, by substitution (like in the case of covalently inherently chiral resorcinarenes)[5,17] or by asymmetric positions of the hydrogens (like in the present "noncovalent" case, Figure 6b,c). In order to predict the direction of the electric dipole of the lowest ^1L_b electronic transition, the ab initio calculation of the simple resorcinol chromophore with an asymmetric OH geometry was preformed (Figure 6b). The TDDFT calculations at the B3LYP/DZVP level indicate that the lowest-energy transition at 247 nm has HOMO→LUMO and HOMO–1→LUMO+1 components. The electric dipole connected with that transition is polarized in the plane of the resorcinol ring (*xy*). In addition to the relatively large *y* component, the asymmetry of the OH groups is responsible for the small *x* component of that electrical moment. This causes the turn of the electric dipole (the angle is +4°, Figure 6b). The magnetic dipole of that transition is perpendicular to the resorcinol ring exhibiting only *z* contribution. The additional calculations using the B3LYP functional and 6-31+(d,p) basis set gave a UV spectrum almost identical to that generated by using the DZVP basis set. In this case, the lowest-energy transition (also at 247 nm) had HOMO→LUMO and HOMO–1→LUMO+3 components. Although the orbital numbering (and order) is different, the shape of the orbitals involved in the transition at 247 nm is identical. Thus, the orientation of the electric-transition dipoles is the same as that calculated by using the DZVP basis set.

For the spatial arrangement of the four asymmetric resorcinol rings like in (*P*)-**6** and (*P*)-**7** (Figure 6d) and with relatively small *α* angles, all possible combinations of two

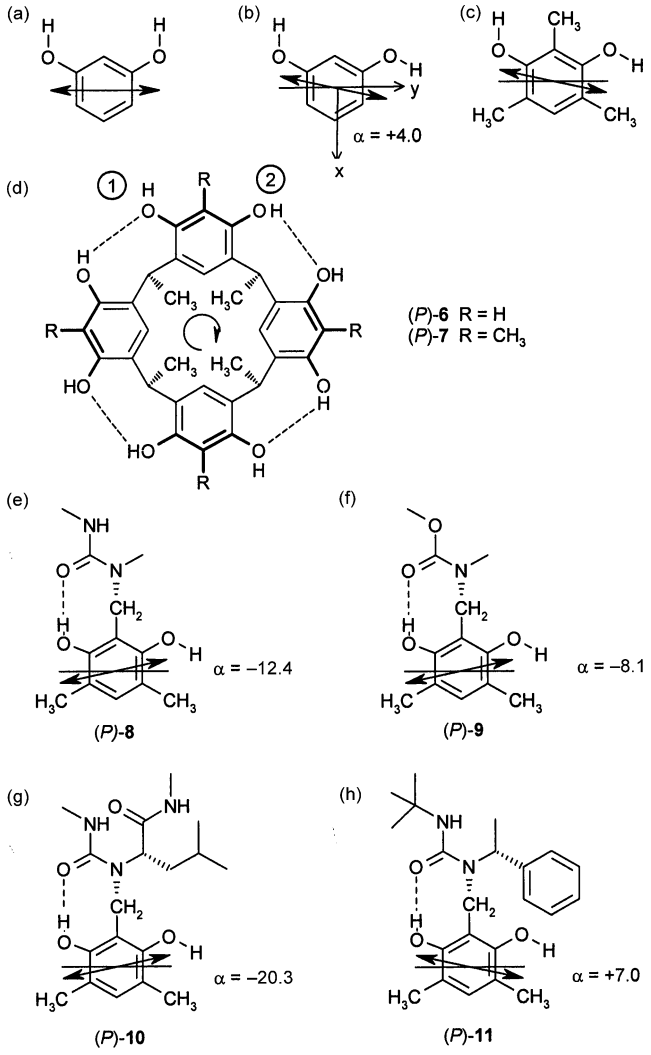

Figure 6. Model compounds for the ab initio calculations. Arrows indicate the directions of the electric dipole moments for the lowest-energy transitions as calculated by TDDFT/B3LYP/DZVP.

electric-transition dipoles are characterized by the positive torsion angles (See Supporting Information). This, according to the *exciton chirality rule*, should result in a positive CD couplet.

To check those predictions, we also preformed the ab initio calculations by using TDDFT/CAMB3LYP/6-31++G* and TDDFT/B3LYP/DZVP for the model tetramers (*P*)-**6** and (*P*)-**7** [both having formal (*P*) arrangement of the hydrogen-bonding system, in analogy to **5b**, Figure 6d]. In the case of (*P*)-**6**, geometry optimization resulted in the C_4-symmetric cone conformation being the energy minimum. Interestingly, in the case of (*P*)-**7**, the C_4-cone conformation appeared to be a "saddle" point, indicating a transition state. However, because both structures are only models to evaluate the influence of the inherent chirality of the hydrogen-bonding system, we calculated the CD spectra for both structures. The comparison of the results for those two basis sets with experimental data leads to the conclusion that the DZVP basis set reproduces the band energy better than

6-31++G*. However, both calculations gave the same CD qualitative result: the strong positive CD couplet for the lowest-energy bands for both (*P*)-**6** and (*P*)-**7** (Figure 7).

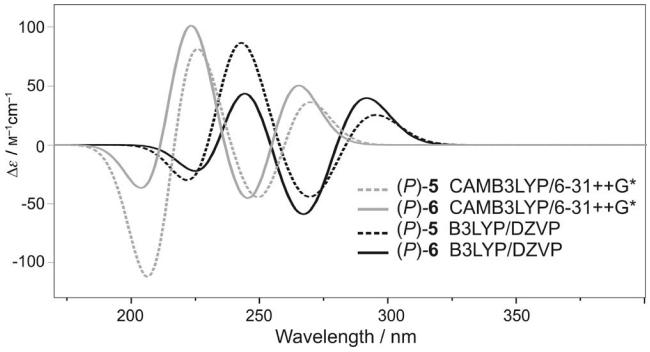

Figure 7. Calculated CD spectra for (*P*)-**6** and (*P*)-**7**.

Although the ab initio calculations and the exciton coupling theory produced consistent results and indicated that a chiral hydrogen-bonding system can produce a considerable CD signal, these predictions are in contradiction to our experimental observations for **5b** with respect to the sign of the couplet. Although, it is known that the theoretical calculations with approximate models as those we employed may give erroneous results for the ECD spectra, we believe that in our case the difference comes from the additional interactions with the remaining part of the molecule or solvent molecules that were not taken into account during the calculations.

In order to evaluate the influence of additional groups and chromophores on the transitions under discussion, we preformed ab initio calculations for monomeric fragments "(*P*)"-**8** and "(*P*)"-**9**, which are the simplest monomers containing additional chromophores. Their starting geometries were derived from the crystal structures (previously reported[6] or current). Upon geometry optimization, the molecular shape of those fragments underwent only minor changes in relation to their crystal structures. The TDDFT/B3LYP/DZVP calculations for monomers "(*P*)"-**8** and "(*P*)"-**9** showed a well-separated low-energy transition at 263 nm (next transition ca. 226 nm), which had HOMO→LUMO and HOMO–1→LUMO+1 components. The analysis of the orbitals involved in those transitions (see Supporting Information) indicates that the urea chromophore also has a slight contribution to those orbitals. As a result, the electric-transition dipole has the *opposite turn* in comparison to that of a simple resorcinol with the same asymmetric position of the OH groups.

Monomer "(*P*)"-**10** is the monomeric fragment of the crystal structure (*P*)-**5b**. In addition to the urea-type chromophore, it contains yet another chromophore that can interfere with the transition of interest − an amide group from the amino acid backbone. The TDDFT/B3LYP/DZVP calculations showed that all chromophores have some contributions to the lowest-energy transition at 263 nm. In this case, the electric-transition dipole is also polarized in the plane of the resorcinol ring, having the same turn as the cases with urea-type chromophores. It is noteworthy that the turn angle is the largest in the current case (α = –20.3°). Thus, for such an orientation of the electric-transition dipole, the *exciton chirality rule* predicts the *negative* sign of the couplet − in agreement with the experimental observation.

For the monomer "(*P*)"-**11**, which is the fragment of the previously reported crystal structure of (*P*)-**5f**,[6] the potential disturbance of the transition of interest can also come from a phenyl ring residing in close proximity to the resorcinol. Indeed, the TDDFT/B3LYP/DZVP calculations indicated the crucial contribution of the neighboring phenyl ring in the lowest-energy transitions. The resulting electric-transition dipole has the same turn as that of the simple resorcinol with asymmetric OH groups. Thus, the *exciton chirality rule* predicts a positive couplet for the (*P*) arrangement of the hydrogen-bonding system − as it is indeed observed for the solution and solid sample [crystals of (*P*)-**5f** in KBr].

Although our experimental UV and CD spectra were very similar for aromatic versus aliphatic amino acids, esters versus amides, and even amino acid derivatives versus simple amines, the ab initio calculations indicated that additional chromophores have crucial influence on the transitions in the resorcin[4]arene skeleton. Determination of those contributions combined with the exciton coupling theory allowed the correct prediction of the sign of the couplets for **5b** and **5f**. However, it should be noted that as a result of symmetry reasons, the magnetic-transition dipole, neglected by *exciton chirality methods*, may also need attention.

Conclusions

We prepared amino acid substituted conformationally chiral resorcinarenes in an efficient two-step synthesis. Compounds **5a**–**e** fold into C_4-symmetric conformations due to the formation of chiral seams of hydrogen bonds. The seams can be directed in one particular direction because of diastereomeric conformational preferences (*de* > 95%). The formation of such chiral arrangements is responsible for pronounced effects in the chiroptical spectra. Detailed NMR spectroscopic and X-ray studies allowed the determination of the absolute conformation for **5b** and thus the correlation between the direction of the hydrogen-bonding seam and CD spectra. Thus, with **5b** having a (*P*) arrangement of the hydrogen-bonding system, we observed a negative couplet in the range 280–310 nm. The ab initio calculations for model compounds showed that the chiral arrangement of the hydrogen bonding in resorcinarenes can produce substantial CD effects, which are amplified by exciton coupling. However, it was also shown that the neighboring urea, amide, or phenyl groups have crucial effects on the direction of the electric-transition dipole and, as the result, on the sign of the exciton coupled band.

Experimental Section

General: All chemicals were used as received unless otherwise noted. Reagent-grade solvents (CH_2Cl_2, hexanes) were distilled

prior to use. All reported NMR spectra were collected with a Bruker spectrometer at 500 (^{1}H) and 125 (^{13}C) MHz. Chemical shifts are reported as δ values relative to the TMS signal defined at δ = 0.00 ppm (^{1}H) or relative to the $CDCl_3$ signal defined at δ = 77.00 ppm (^{13}C). Mass spectra were obtained with a Mariner PerSeptive Biosystem instrument by using the ESI technique. Column chromatography was performed on silica gel (Kieselgel 60, 200–400 mesh).

4a: Resorcinarene **2** (712 mg, 1 mmol) and L-leucine methylamide (720 mg, 5 mmol) were dissolved in CH_2Cl_2 (5 mL). Aqueous HCHO was then added (37%, 300 μL, 4.0 mmol). The reaction mixture was vigorously stirred overnight at room temperature. The reaction mixture was evaporated to dryness, and the crude product was purified by column chromatography (CH_2Cl_2/MeOH, 97:3 to 95:5). Subsequent crystallization from CH_2Cl_2 gave **4a** as a white crystalline material (856 mg, 64%). $[\alpha]_D$ = –4.0 (c = 1.0, MeOH). ^{1}H NMR (400 MHz, DMSO, TMS, 303 K): δ = 0.83 (d, J = 6.6 Hz 12 H), 0.85 (d, J = 6.5 Hz 12 H), 0.89 (d, J = 6.8 Hz 12 H), 0.91 (d, J = 6.9 Hz 12 H), 1.36 (m, 12 H), 1.55 (m, 4 H), 1.98 (m, 4 H), 2.13 (m, 4 H), 2.60 (d, J = 4.6 Hz, 12 H, H^l), 3.09 (t, J = 7.1 Hz, 4 H, H^g), 3.54 (d, J = 15.0 Hz, 4 H, H^f), 3.87 (d, J = 15.0 Hz, 4 H, H^f), 4.25 (t, J = 7.6 Hz, 4 H, H^d), 7.19 (s, 4 H, H^e), 8.02 (br. q, J = 4.8 Hz, 4 H, H^k) ppm. ^{13}C NMR (100 MHz, DMSO, 303 K): δ = 22.26, 22.65, 22.78, 22.96, 24.21, 25.40, 25.80, 30.76, 41.47, 41.65, 43.69, 58.53, 108.02, 122.37, 123.37, 123.60, 151.23, 151.72, 172.31 ppm. MS (ESI): m/z = 1335.9 $[C_{88}H_{112}N_8O_{12} - H]^-$; isotope profile agrees. $C_{76}H_{120}N_8O_{12}\cdot 0.9CH_2Cl_2$ (1414.25, solvent visible also in NMR): calcd. C 65.31, H 8.68, N 7.92; found C 65.30, H 8.85, N 8.02.

4b: To a solution of resorcinarene **2** (712 mg, 1 mmol) and L-phenylalanine methylamide (890 mg, 5 mmol) in CH_2Cl_2 (5 mL) was added aqueous HCHO (37%, 300 μL, 4.0 mmol). The reaction mixture was vigorously stirred overnight at room temperature. The resulting precipitate was filtered, washed with CH_2Cl_2 and water, and then vacuum dried to give analytically pure **4b** as a pinkish powder (1.120 g, 76%). $[\alpha]_D$ = +2.5 (c = 1.16, MeOH). ^{1}H NMR (400 MHz, DMSO, TMS, 303 K): δ = 0.89 (m, 24 H, H^a), 1.31 (m, 4 H, H^b), 1.95 (m, 4 H, H^c), 2.03 (m, 4 H, H^c), 2.55 (d, J = 4.6 Hz, 12 H, H^l), 2.70 (dd, J = 13.4 Hz, J = 8.1 Hz, 4 H, H^{h1}), 2.83 (dd, J = 13.4 Hz, J = 5.7 Hz, 4 H, H^{h2}), 3.28 (t, J = 6.9 Hz, 4 H, H^g), 3.52 (d, J = 14.7 Hz, 4 H, H^{f2}), 3.88 (d, J = 14.7 Hz, 4 H, H^{f1}), 4.09 (t, J = 7.6 Hz, 4 H, H^d), 7.12–7.28 (m, 24 H, H^e, H^i), 7.95 (br. q, J = 4.7 Hz, 4 H, H^k) ppm. ^{13}C NMR (100 MHz, DMSO, 303 K): δ = 22.72, 22.85, 25.34, 25.79, 30.61, 41.52, 43.48, 54.52, 61.86, 108.45, 122.37, 123.33, 123.50, 126.22, 128.12, 129.14, 137.58, 150.99, 171.91 ppm. MS (ESI): m/z = 1472.6 $[C_{88}H_{112}N_8O_{12} - H]^-$; isotope profile agrees. $C_{88}H_{112}N_8O_{12}\cdot 0.8CH_2Cl_2$ (1541.8, solvent visible also in NMR): calcd. C 69.17, H 7.42, N 7.27; found C 69.10, H 7.38, N 7.15.

5a: To a solution of amine **4a** (267 mg, 0.2 mmol) in dioxane/water (2:1, 3 mL) was added Boc_2O (348 mg, 1.6 mmol). The reaction mixture was stirred overnight and evaporated to dryness. The crude product was purified by column chromatography (CH_2Cl_2/MeOH, 99:1) to give **5a** as an off-white powder (220 mg, 63%). $[\alpha]_D^{25}$ = –111.3 (c = 1.20, $CHCl_3$). ^{1}H NMR (500 MHz, $CDCl_3$, TMS, 303 K): δ = 0.93 (m, 24 H, H^j), 0.96 (d, J = 2.2 Hz, 12 H, H^a), 0.98 (d, J = 2.2 Hz, 12 H, H^a), 1.42 (br. s, 40 H, H^b, H^m), 1.56 (m, 4 H, H^i), 1.82–1.98 (m, 8 H, H^h), 2.09 (m, 8 H, H^c), 2.53 (br. s, 12 H, H^l), 4.26 (d, J = 14.8 Hz, 4 H, H^{f2}), 4.31 (m, 4 H, H^g), 4.56 (t, J = 7.5 Hz, 4 H, H^d), 4.57 (d, J = 14.8 Hz, 4 H, H^{f1}), 5.34 (br. s, 4 H, H^k), 7.21 (s, 4 H, H^e), 8.55 (br. s, 4 H, OH^2), 10.77 (br. s, 4 H, OH^1) ppm. ^{13}C NMR (125 MHz, $CDCl_3$, 303 K): δ = 22.16, 22.57, 22.63, 23.55, 25.00, 26.03, 26.39, 27.40, 28.17, 31.70, 38.44, 42.79, 61.65, 82.90, 85.13, 112.30, 124.06, 124.95, 125.08, 149.78, 151.35, 158.13, 171.89 ppm. MS (ESI): m/z = 1736.2 $[C_{96}H_{152}N_8O_{20} - H]^-$; isotope profile agrees. $C_{96}H_{152}N_8O_{20}\cdot 2MeOH$ (1802.36): calcd. C 65.30, H 8.95, N 6.21; found C 65.34, H 8.96, N 6.00.

5b: To a solution of amine **4a** (267 mg, 0.2 mmol) in THF (2 mL) was added *tert*-butyl isocyanate (242 μL, 2 mmol). The reaction mixture was stirred overnight and evaporated to dryness. The crude product was purified by column chromatography (CH_2Cl_2/MeOH, 99:1) to give **5b** as an off-white powder (180 mg, 52%). $[\alpha]_D^{25}$ = +81.5 (c = 0.99, $CHCl_3$). ^{1}H NMR (500 MHz, [D$_2$]TCE, 303 K) main conformer: δ = 0.40 (br. s, 12 H, H^j), 0.73 (br. s, 12 H, H^j), 0.93 (br. s, 12 H, H^a), 0.99 (d, J = 5.5 Hz, 12 H, H^a), 1.07 (br. m, 4 H, H^i), 1.40 (s, 40 H, H^m, H^h), 1.47 (m, 4 H, H^b), 1.71 (s, 4 H, H^h), 1.76 (br. m, 4 H, H^c), 2.25 (br. m, 4 H, H^c), 2.94 (br. s, 12 H, H^l), 3.74 (br. s, 4 H, H^g), 4.31 (br. d, H^{f2}), 4.44 (br. d, 4 H, H^{f1}), 4.53 (br. t, 4 H, H^d), 6.37 (br. t, 4 H, H^k), 7.18 (s, 4 H, H^e), 7.86 (br. s, 4 H, H^n), 8.60 (br. s, 4 H, OH^2), 12.13 (br. s, 4 H, OH^1) ppm. ^{13}C NMR (125 MHz, [D$_2$]TCE, 303 K): δ = 25.40, 26.13, 26.60, 26.95, 27.26, 28.14, 29.82, 30.71, 33.31, 33.58, 35.43, 42.06, 46.45, 46.76, 54.53, 63.0 (broad), 115.31, 127.65, 128.18, 128.81, 154.26, 154.80, 163.45, 177.12 ppm. MS (ESI): m/z = 1732.1 $[C_{96}H_{156}N_{12}O_{16} - H]^-$; isotope profile agrees. $C_{96}H_{156}N_{12}O_{16}$ (1734.34): calcd. C 66.48, H 9.07, N 9.69; found C 66.24, H 9.03, N 9.53.

5c: According to the procedure described for **5a**. Yield 281 mg, 75%. $[\alpha]_D^{25}$ = –124.1 (c = 1.00, $CHCl_3$). ^{1}H NMR (500 MHz, [D$_2$]-TCE, 303 K): δ = 0.94 (br. d, 24 H, H^a), 1.35 (m, 4 H, H^b), 1.50 (s, 36 H, H^m), 2.01 (br. s, 8 H, H^c), 2.58 (br. s, 12 H, H^l), 3.21 (m, 4 H, H^{h1}), 3.39 (m, 4 H, H^{h2}), 3.46 (br. s, 4 H, H^{f2}), 4.05 (d, J = 14.0 Hz, 4 H, H^{f1}), 4.45 (br. t, 4 H, H^d), 4.59 (m, 4 H, H^g), 5.29 (br. s, 4 H, H^k), 7.08 (s, 4 H, H^e), 7.18 (br. m, 20 H, $H^{i\text{-}ar}$), 8.22 (s, 4 H, OH^2), 10.53 (s, 4 H, OH^1) ppm. ^{13}C NMR (125 MHz, $CDCl_3$, 303 K): δ = 22.50, 22.63, 26.07, 26.37, 28.29, 31.56, 35.07, 42.79, 45.50, 65.07, 83.11, 112.35, 123.83, 124.86, 125.08, 126.41, 128.55, 129.22, 138.46, 149.47, 151.11, 157.89, 171.13 ppm. ^{15}N NMR (50.7 MHz, $CDCl_3$): δ = –289.1 (NH) ppm. MS (ESI): m/z = 1896.2 $[C_{108}H_{144}N_8O_{20} + Na]^+$, 1872.3 $[C_{108}H_{144}N_8O_{20} - H]^-$; isotope profile agrees. $C_{108}H_{144}N_8O_{20}$ (1874.34): calcd. C 69.21, H 7.74, N 5.98; found C 68.90, H 7.69, N 6.13.

5d: According to the procedure described for **5b**. Yield 221 mg, 59%. $[\alpha]_D^{25}$ = –42.5 (c = 1.00, $CHCl_3$). ^{1}H and ^{13}C NMR spectra were too broad for interpretation. MS (ESI): m/z = 1869.1 $[C_{108}H_{148}N_{12}O_{16} - H]^-$, 1893.2 $[C_{108}H_{148}N_{12}O_{16} + Na]^+$; isotope profile agrees. $C_{108}H_{148}N_{12}O_{16}\cdot 2H_2O$ (1906.43): calcd. C 68.04, H 8.04, N 8.81; found C 68.08, H 8.03, N 9.05.

5e: To a solution of amine **4a** (267 mg, 0.2 mmol) in THF (2 mL) was added trimethylsilyl isocyanate (280 μL, 2 mmol). The reaction was stirred for 3 d and then evaporated to dryness and suspended in acetone (2 mL). The mixture was heated at reflux for 5 min and then left for 2 h to precipitate. The analytically pure **5e** (as a pinkish powder) was obtained by filtration (217 mg, 66%). An alternative procedure involves solvent change from THF to methanol. It allows shortening of the reaction time to 1 d (216 mg, 66%). $[\alpha]_D^{25}$ = –86.8 (c = 1.00, $CHCl_3$). ^{1}H NMR (500 MHz, $CDCl_3$, TMS, 303 K): δ = 0.91 (d, J = 6.6 Hz, 12 H, H^a), 0.96 (d, J = 6.4 Hz, 12 H, H^a), 1.44 (br. m, 4 H, H^b), 1.85 (br. m, 4 H, H^{c1}), 2.17 (br. m, 4 H, H^{c2}), 2.70 (br. d, J = 4.5 Hz, 12 H, H^l), 3.14 (dd, J = 5.7 Hz, J = 13.8 Hz, 4 H, H^{h1}), 3.41 (dd, J = 13.0 Hz, J = 10.5 Hz, 4 H, H^{h2}), 3.47 (d, J = 15.5 Hz, 4 H, H^{f2}), 4.24 (d, J = 15.2 Hz, 4 H, H^{f1}), 4.47 (br. t, J = 7.8 Hz, 4 H, H^d), 4.52 (m, 4 H, H^g), 6.00 (br. s, 8 H, H^n), 7.06 (s, 4 H, H^e), 7.26–7.37 (m, 20 H, H^i), 7.47 (br. q,

4 H, H^k), 9.19 (s, 4 H, OH^2), 11.77 (s, 4 H, OH^1) ppm. ^{13}C NMR (125 MHz, $CDCl_3$, 303 K): δ = 22.51, 23.39, 25.99, 26.30, 31.93, 34.25, 42.35, 48.43, 66.43, 114.49, 123.39, 125.26, 126.67, 126.94, 128.79, 129.28, 136.95, 149.45, 150.08, 160.79, 171.24 ppm. MS (ESI): m/z = 1644.9 $[C_{92}H_{116}N_{12}O_{16} - H]^-$, 1668.0 $[C_{92}H_{11}N_{12}O_{16} + Na]^+$; isotope profile agrees. $C_{92}H_{116}N_{12}O_{16}\cdot 2H_2O$ (1682.01): calcd. C 65.69, H 7.19, N 9.99; found C 65.68, H 6.95, N 10.07.

UV/Vis and CD Spectroscopy: CD spectra were measured at room temperature with solutions (solvents UV grade) at concentrations of ca. 10^{-4} M with a Jasco 715 spectrophotometer by using cells with path length 0.1 to 1 cm (spectral band width 2 nm, sensitivity 5×10^{-6} or 10×10^{-6} [ΔA unit nm^{-1}], where $\Delta A = A_L - A_R$ is the difference in the absorbance). $\Delta\varepsilon$ is expressed in [L mol^{-1} cm^{-1}]. Solid-state samples were obtained by grinding of the respective crystals (the same as used for X-ray structure determination) in a KBr matrix. The measurements for solid state samples were qualitative.

X-ray Crystallographic Structure Determination of 5b: The diffraction quality crystals of **5c** were grown from CH_2Cl_2/MeCN solution. After removal from the mother liquid the crystal was immediately covered with an immersion oil and frozen at 153 K. The measurement was performed with a KM4CCD j-axis diffractometer with graphite-monochromated Mo-K_α radiation. The crystal was positioned at 62 mm from the CCD camera. 1500 Frames were measured at 0.5° intervals with a counting time of 30 s. The data were corrected for Lorentz and polarization effects. Data reduction and analysis were carried out with the Oxford Diffraction programs. The structure was solved with DIRDIF by using the resorcinarene skeleton as a starting structure for ORIENT.[18] The crystal was twinned by merohedry (twinning matrix 1 0 0 0 –1 0 –1 0 –1, occupancy 0.67: 0.33). The structure was refined by using SHELXL (X-Seed interface)[19] against twinned data. The refinement was based on F^2 for all reflections except those with very negative F^2. Weighted R factors wR and all goodness-of-fit S values are based on F^2.The non-hydrogen atoms were refined with anisotropic thermal parameters, and all H atoms were positioned geometrically. The geometrical restraints were applied for disordered atoms. $C_{108}H_{174}N_{18}O_{16}$, M = 1980.65, monoclinic, space group $P2_1$ (No. 4), a = 9.0772(6) Å, b = 35.982(2) Å, c = 18.555(1) Å, β = 103.712(5)°, V = 5887.7(6) Å^3, Z = 2, $D_{calcd.}$ = 1.117 g/cm^3, $F(000)$ = 2152, Mo-K_α radiation, λ = 0.71073 Å, T = 173(2) K, $2\theta_{max}$ = 57.6°, 110241 reflections collected, 28245 unique (R_{int} = 0.0514). Final $GooF$ = 0.932, R_1 = 0.0510, wR_2 = 0.1123, R indices based on 19958 reflections with $I > 2\sigma(I)$ (refinement on F^2), 1369 parameters, 1 restraint. Lp and absorption corrections applied, μ = 0.076 mm^{-1}.

CCDC-676741 contains the supplementary crystallographic data for this paper. These data can be obtained free of charge from The Cambridge Crystallographic Data Centre via www.ccdc.cam.ac.uk/data_request/cif.

Computational Details: The structures of model compounds were optimized by means of DFT with the B3LYP functional and 6-31G* basis set. The CD spectra were calculated by using time-dependent DFT[20] with B3LYP (or CAMPB3LYP) functional and DZVP (or 6-31++G*) basis set. Both the length gauge formulation with London orbitals and velocity gauge formulation were used, and the differences between the two sets of results were negligible. The ab initio calculations were preformed by using Gaussian 03[21] and Dalton[22] software.

Supporting Information (see footnote on the first page of this article): NMR spectra of **5a**–**e**; additional figures for graphical representation of vectors for (*P*)-**6** and molecular orbitals for (*P*)-**8**.

Acknowledgments

This work was supported by the Ministry of Science and Higher Education (Project # N20408631/2028 and 1TO9A07130). We are grateful to Prof. Jadwiga Frelek and her group members for kind assistance with the CD measurements. The X-ray data collection was undertaken at the Crystallographic Unit of the Physical Chemistry Laboratory, Chemistry Department, University of Warsaw.

[1] D. S. Goodsell, A. J. Olson, *Ann. Rev. Biophys. Biomol. Struct.* **2000**, *29*, 105–153.
[2] D. Bray, T. Duke, *Ann. Rev. Biophys. Biomol. Struct.* **2004**, *33*, 53–73.
[3] a) T. Ooi, K. Maruoka, *Aldrichimica Acta* **2007**, *40*, 77–86; b) G. Desimoni, G. Faita, K. A. Jorgensen, *Chem. Rev.* **2006**, *106*, 3561–3651; c) S. Castillon, C. Claver, Y. Diaz, *Chem. Soc. Rev.* **2005**, *34*, 702–713; d) S. E. Gibson, M. P. Castaldi, *Angew. Chem. Int. Ed.* **2006**, *45*, 4718–4720; e) S. E. Gibson, M. P. Castaldi, *Chem. Commun.* **2006**, 3045–3062; f) C. Moberg, *Angew. Chem. Int. Ed.* **1998**, *37*, 248–268; g) J. Zhou, M. C. Ye, Z. Z. Huang, Y. Tang, *J. Org. Chem.* **2004**, *69*, 1309–1320.
[4] A. R. A. Palmans, E. W. Meijer, *Angew. Chem. Int. Ed.* **2007**, *46*, 8948.
[5] a) M. Paletta, M. Klaes, B. Neumann, H. G. Stammler, S. Grimme, J. Mattay, *Eur. J. Org. Chem.* **2008**, 555–562; b) M. Klaes, C. Agena, M. Kohler, M. Inoue, T. Wada, Y. Inoue, J. Mattay, *Eur. J. Org. Chem.* **2003**, 1404–1409; c) R. Arnecke, V. Böhmer, E. F. Paulus, W. Vogt, *J. Am. Chem. Soc.* **1995**, *117*, 3286–3287; d) P. C. B. Page, H. Heaney, E. P. Sampler, *J. Am. Chem. Soc.* **1999**, *121*, 6751–6752; e) W. Iwanek, J. Mattay, *Liebigs Ann.* **1995**, 1463–1466; f) M. T. El Gihani, H. Heaney, A. M. Z. Slawin, *Tetrahedron Lett.* **1995**, *36*, 4905–4908; g) R. Arnecke, V. Böhmer, S. Friebe, S. Gebauer, G. J. Krauss, I. Thondorf, W. Vogt, *Tetrahedron Lett.* **1995**, *36*, 6221–6224; h) J. Luo, Q.-Y. Zheng, C.-F. Chen, Z.-T. Huang, *Chem. Eur. J.* **2005**, *11*, 5917–5928; i) R. Mao, Q.-Y. Zheng, C.-F. Chen, Z.-T. Huang, *J. Org. Chem.* **2005**, *70*, 7662–7671; j) J. Luo, Q.-Y. Zheng, C.-F. Chen, Z.-T. Huang, *Tetrahedron* **2005**, *61*, 8517–8528; k) Z.-X. Xu, C. Zhang, Q.-Y. Zheng, C.-F. Chen, Z.-T. Huang, *Org. Lett.* **2007**, *9*, 4447–4450; l) Z.-X. Xu, C. Zhang, Y. Yang, C.-F. Chen, Z.-T. Huang, *Org. Lett.* **2008**, *10*, 477–479.
[6] A. Szumna, *Org. Biomol. Chem.* **2007**, *5*, 1358–1368; see also corrections.
[7] a) D. M. Rudkevich, G. Hilmersson, J. Rebek, *J. Am. Chem. Soc.* **1997**, *119*, 9911–9912; b) S. Saito, C. Nuckolls, J. Rebek, *J. Am. Chem. Soc.* **2000**, *122*, 9628–9630; c) A. Shivanyuk, K. Rissanen, S. K. Korner, D. M. Rudkevich, J. Rebek, *Helv. Chim. Acta* **2000**, *83*, 1778–1790; d) C. Schmidt, E. F. Paulus, V. Böhmer, W. Vogt, *New J. Chem.* **2000**, *24*, 123–125; e) M. Luostarinen, M. Nissinen, M. Nieger, A. Shivanyuk, K. Rissanen, *Tetrahedron* **2007**, *63*, 1254–1263.
[8] M. Klaes, B. Neumann, H. G. Stammler, J. Mattay, *Eur. J. Org. Chem.* **2005**, 864–868.
[9] a) G. Toth, C. R. Watts, R. F. Murphy, S. Lovas, *Protein Struct. Funct. Genet.* **2001**, *43*, 373–381; b) L. Bendova, P. Jurecka, P. Hobza, J. Vondrasek, *J. Phys. Chem. B* **2007**, *111*, 9975–9979.
[10] B. R. Buckley, J. Y. Boxhall, P. C. B. Page, Y. Chan, M. R. J. Elsegood, H. Heaney, K. E. Holmes, M. J. McIldowie, V. McKee, M. J. McGrath, M. Mocerino, A. M. Poulton, E. P. Sampler, B. W. Skelton, A. H. White, *Eur. J. Org. Chem.* **2006**, 5117–5134.
[11] C. Schiel, G. A. Hembury, V. V. Borovkov, M. Klaes, C. Agena, T. Wada, S. Grimme, Y. Inoue, J. Mattay, *J. Org. Chem.* **2006**, *71*, 976–982.
[12] a) E. Castiglioni, S. Abbate, G. Longhi, R. Gangemi, *Chirality* **2007**, *19*, 491–496; b) R. Kuroda, T. Honma, *Chirality* **2000**, *12*, 269–277.

[13] A. Szumna, M. Gorski, O. Lukin, *Tetrahedron Lett.* **2005**, *46*, 7423–7426; Supporting Information
[14] J. Frelek, P. Kowalska, M. Masnyk, A. Kazimierski, A. Korda, M. Woznica, M. Chmielewski, F. Furche, *Chem. Eur. J.* **2007**, *13*, 6732–6744.
[15] S. Allenmark, *Chirality* **2003**, *15*, 409–422.
[16] a) N. Berova, L. Di Bari, G. Pescitelli, *Chem. Soc. Rev.* **2007**, *36*, 914–931; b) H. W. Liu, K. Nakanishi, *J. Am. Chem. Soc.* **1981**, *103*, 5591–5593; c) H. W. Liu, K. Nakanishi, *J. Am. Chem. Soc.* **1982**, *104*, 1178–1185; d) N. Harada, K. Nakanishi, *Circular Dichroic Spectroscopy – Exciton Coupling in Organic Stereochemistry*, Oxford University Press, Oxford, **1983**; e) N. Berova, N. Harada, K. Nakanishi, "Electronic Spectroscopy: Exciton Coupling, Theory, Applications" in *Encyclopedia of Spectroscopy, Spectrometry* (Eds.: J. Lindon, G. Tranter, J. Holmes), Academic Press, New York, **2000**.
[17] B. R. Buckley, P. C. B. Page, Y. Chan, H. Heaney, M. Klaes, M. J. McIldowie, V. McKee, J. Mattay, M. Mocerino, E. Moreno, B. W. Skelton, A. H. White, *Eur. J. Org. Chem.* **2006**, 5135–5151.
[18] a) P. T. Beurskens, G. Beurskens, R. de Gelder, S. Garcia–Granda, R. O. Gould, R. Israel, J. M. M. Smits, *The DIRDIF–99 Program System*, Crystallography Laboratory, University of Nijmegen, The Netherlands; b) V. Parthasarathi, P. T. Beurskens, H. J. Bruins Slot, *Acta Crystallogr., Sect. A* **1983**, *39*, 860–864.
[19] L. J. Barbour, *J. Supramol. Chem.* **2001**, *1*, 189–191.
[20] a) K. L. Bak, A. E. Hansen, K. Ruud, T. Helgaker, J. Olsen, P. Jorgensen, *Theor. Chim. Acta* **1995**, *90*, 441–458; b) M. Pecul, K. Ruud, T. Helgaker, *Chem. Phys. Lett.* **2004**, *388*, 110–119.
[21] *Gaussian 03*, Revision B.05, Gaussian, Inc., Pittsburgh, PA, **2003**.
[22] *Dalton, An Ab Initio Electronic Structure Program*, release 2.0, **2005**. See http://www.kjemi.uio.no/software/dalton/dalton.html.

Received: March 5, 2008
Published Online: April 29, 2008

